processes

MDPI

Review

Terpene Based Elastomers: Synthesis, Properties, and Applications

Pranabesh Sahu [1], Anil K Bhowmick [1,2,*] and Gergely Kali [3,*]

[1] Rubber Technology Centre, Indian Institute of Technology Kharagpur, Kharagpur 721302, India; pranabesh.cema@gmail.com
[2] Department of Chemical and Biomolecular Engineering, University of Houston, Houston, TX 77204, USA
[3] Center for Chemistry and Biomedicine, Department of Pharmaceutical Technology, Institute of Pharmacy, University of Innsbruck, Innrain 80/82, 6020 Innsbruck, Austria
* Correspondence: anilbhowmick@gmail.com (A.K.B.); gergelykali@gmail.com (G.K.)

Received: 13 April 2020; Accepted: 2 May 2020; Published: 8 May 2020

Abstract: The limited source of fossil-fuel and the predominance of petroleum-based chemistry in the manufacturing of commodity polymers has generated tremendous interest in replacing the fossil source-based polymers with renewable counterparts. The field of sustainable elastomers has grown in the past three decades, from a few examples to a plethora of reports in modern polymer science and technology. Applications of elastomers are huge and vital for everyday living. The present review aims to portray a birds-eye view of various sustainable elastomers obtained from the wide family of acyclic terpenes (renewable feedstocks from different plant oils) via various polymerization techniques and their properties, as well as plausible developments in the future applications of sustainable polymers. Not only the homopolymers, but also their copolymers with both green and commercial fossil based comonomers, are reviewed.

Keywords: terpenes; sustainable elastomer; structure-property relationship; properties

1. Introduction

Green chemistry was only a new trend a few decades ago, but it has become an essential and hot topic of research in the last few years because of the significant environmental pollution by fossil resources and their limited future availability. For polymers/plastics, it is especially important because of their large-scale production and a large amount of consumption. Considering the soaring petroleum prices and environmental pollution, the use of petroleum-based products is not an environmentally favorable process. One of the partial solutions for reducing pollution and fossil resource-dependent industrial problems is the use of monomers and polymers from renewable resources. In this situation, we have to utilize this period to evaluate and create major pathways to use alternative resources for the production of biobased synthetic elastomers. Terpenes or terpenoids are natural materials built from isoprene and produced by plants and insects [1,2]. Terpenes are readily available in large amounts and with a variety of structures, and therefore can be easily used for synthesis even without modifications. There are several types of terpenes, based on the number of isoprene units (in brackets) in their structure, such as mono (2), sesqui (3), diterpenes (4), etc., including some polymerizable ones. The directly polymerized terpenes are mainly monoterpenes, for example, myrcene, pinene, or limonene [3–5]. Some other terpenes can be subjected to Baeyer–Villiger oxidation, and the resulting lactone becomes polymerizable via ring-opening methods [5]. There are several polymerization methods applicable to the different terpenes. Radical, ionic, or even coordinative polymerizations of monomeric terpenes are well known [3,5]. Here we will focus on the elastomeric polyterpenes based on mostly myrcene, but other terpenes, such as ocimene, farnesene and alloocimene, will also

be discussed. Their syntheses, properties and commercialized applications—or those that can be marketed in the near future—will be reviewed.

2. Synthesis of Terpene Based Elastomers

One of the most important elastomeric polyterpenes is polyisoprene [6,7]. Natural rubber is an enzymatically produced, highly uniform polyisoprene, but this monomer can also be polymerized by standard radical and ionic polymerization methods, resulting in slightly different products [8,9]. Even industrially, it is the most important elastomer. It is already well described and reviewed, and therefore, we do not want to focus on it.

2.1. Myrcene

Synthetic polyterpenoid elastomers based on monoterpenes are well known. Myrcene is one of the most important terpenoids. Not only because of its broad availability in nature, as well as from industrial synthesis by pinene pyrolysis, but also due to the versatility of the polymerization methods for *β*-myrcene without preliminary modifications [5,10,11]. *β*-Myrcene has been polymerized by radical, anionic, cationic and coordinative methods so far. The formed polymyrcenes of these methods are different in terms of topology, chain length, and also, very importantly, in regioselectivity (Scheme 1). This last property also describes polymer microstructure, which has a massive effect on the properties of the resulting product.

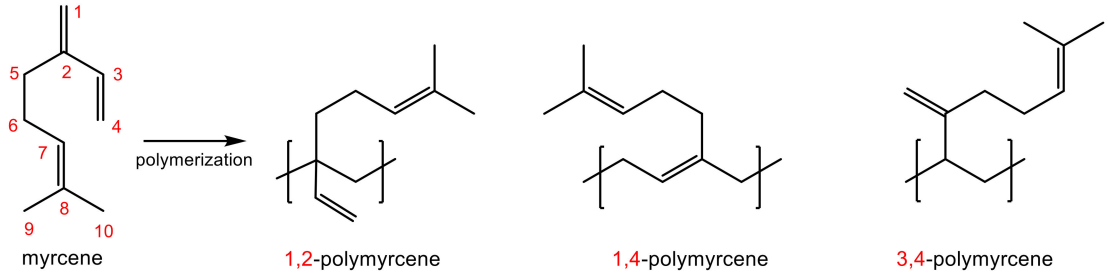

Scheme 1. Schematic representation of the various microstructures of polymeric myrcene.

Free radical polymerization in *n*-butanol, initiated by hydrogen peroxide at around 100 °C, leads to polymyrcene with higher than 75% *1,4*-structure and low dispersity, but with branched/cross-linked side-products because of the reaction of the remaining double bonds and the highly reactive radicals [12–15]. The same radically polymerized myrcene, as well as its polymer synthesized by anionic conditions, was subjected to 3D printing with subsequent thiol-modification, resulting in the formation of superhydrophobic material [16,17]. Emulsion polymerization was also applied to produce polymyrcene, using potassium or ammonium persulfate and *tert*-butyl hydroperoxide initiation, at elevated (60–70 °C) and room temperature, respectively [11,18,19]. The spectra (Figure 1) explain the conversion of the monomer to the polymer. The disappearance of methylene proton peaks in the monomer (C1, C4), and the appearance of broad peaks in the region of 4.50 ppm to 5.50 ppm, suggest the formation of the polymer. The protons of the methyl groups linked to C8 in all the microstructures appear at upfield values of δ = 1.60 ppm and 1.52 ppm, and the methylene protons are displayed as a broad peak at 1.96 ppm. The polymer reported may have four different types of microstructure, viz. *1,4-cis*, *1,4-trans*, *1,2-vinyl* and *3,4*-polymyrcene. Redox starter served a higher portion of *1,4*-microstructures than persulfate analogue, and high molar mass; almost 100 kDa [19]. Vulcanization of the persulfate-initiated polymyrcene led to rubbery materials, with a cross-linking density of 2.50×10^{-4} mol/cm^3, where the formation of the polysulfide linkages was supported by the microstructural defects [20]. Similar to emulsion polymerization, the radical polymerization of *β*-myrcene was also possible with a $K_2S_2O_8/Na_2S_2O_5$ redox initiating system in cyclodextrin solution, where the macrocycle solubilizes the monomer [21].

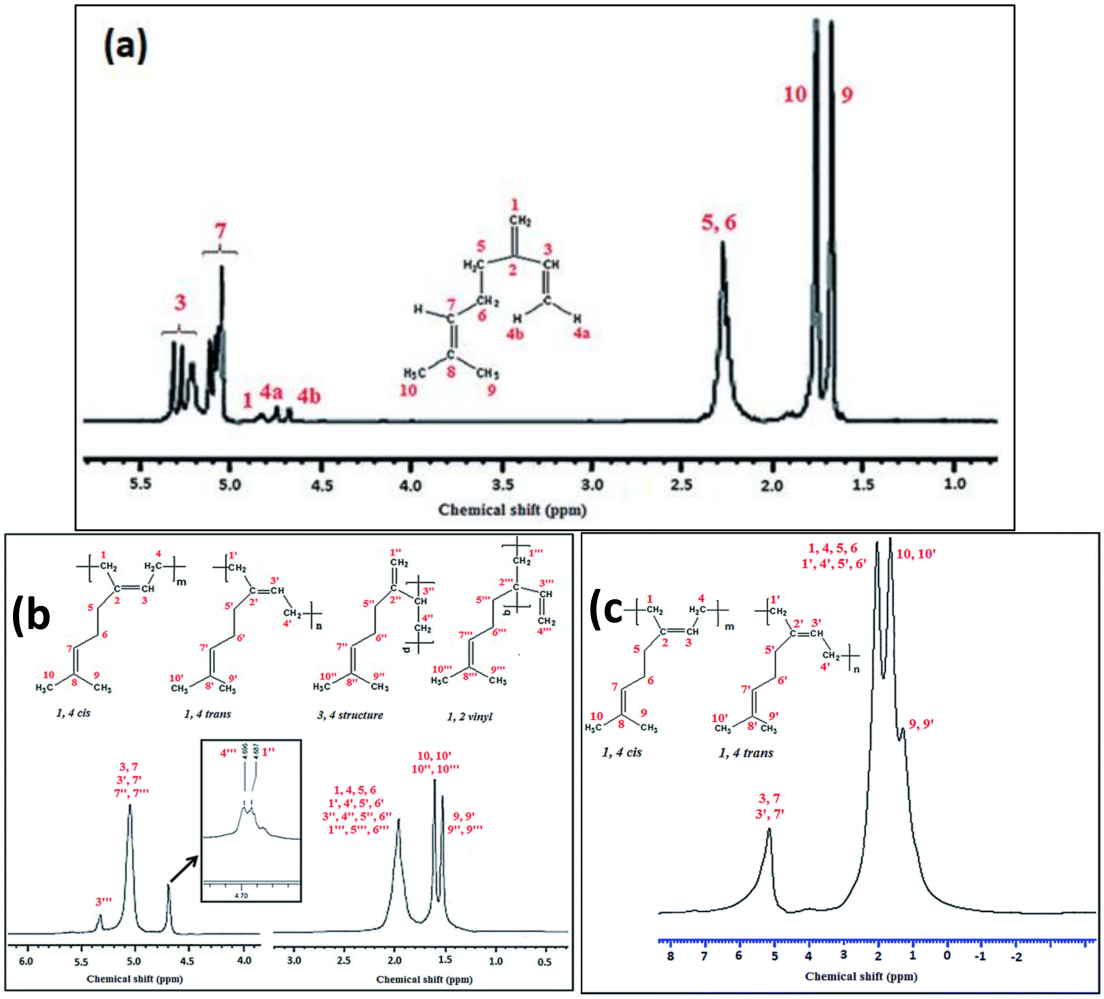

Figure 1. (**a**) ^{1}H NMR spectrum of *β*-myrcene, (**b**) and (**c**) ^{1}H NMR spectra of polymyrcene (persulfate and redox initiated). (Reproduced from Reference 19, with permission from The Royal Society of Chemistry).

This emulsion-like, detergent-free polymerization resulted in low molar mass polymyrcene with dispersity around 2 and mostly 1,4 microstructure. Anionic and cationic polymerizations were carried out using *n*-butyllithium [22–24], boron trifluoride etherate [11,25], and metal halide initiators [26], respectively. The resulting polymers had low dispersity (in all cases Đ ≤ 1.6), high molar masses (up to 30 kDa), and almost quantitative conversion in a short time, but only slightly-regular microstructures (40–90% *1,4*-structures) for anionic polymerization [11,22]. The polymyrcene from the mentioned carbocationic polymerizations consisted of only one double bond per repeating unit, but the exact structure and the mechanism of the reaction were not fully determined. It can be assumed that some intramolecular cyclization could have occurred during the polymerization process [11]. Linear polymyrcene can be produced using *β*-diimidosulfonate lutetium catalyst in carbocationic polymerization, and the produced polymer also has low dispersity (Đ~1.4), as well as high *3,4*-microstructure content [25]. 2-propenyl triflate- or 1-(4-methoxyphenyl) ethyl triflate-initiated cationic polymerization of *β*-myrcene in CH_2Cl_2 and cyclohexane yields oligomeric saturated products [27]. Recently, an aqueous cationic polymerization of *β*-myrcene was carried, out utilizing water-dispersible Lewis acid surfactant combined with ytterbium chloride catalyst at 40 °C [28]. The resulting polymer had molar mass up to 150 kDa, and was rich in *1,4*-microstructure (~93%). Coordinative polymerizations, for example, using Ziegler–Natta type (based on neodymium or lutetium) or lanthanide catalysts, give rise to very high regularity (>98%), but poor polydispersity (Đ ≥ 1.5) [25,29–32]. In a recently described system, cobalt complexes with phenoxy (4,6-di-*tert*-butyl-2-phenol, naphthalene-2-ol)-imine ligands

were used to produce *cis-1,4*-polymyrcene and poly (methyl methacrylate) selectively [33]. Reversible deactivation radical, or so-called controlled radical polymerization, has been applied for the synthesis of this polyterpene in the recent past. This kind of polymerization method is an excellent tool for producing engineered polymers with predetermined properties [34]. Namely, reversible addition-fragmentation chain-transfer polymerization (RAFT) and nitroxide-mediated radical polymerization (NMP) have been successfully applied in such reactions [9,35]. In RAFT polymerization, up to 64% conversion, Đ ≤ 1.6, and even 96% regioregularity, can be reached using 2-ethylsulfanylthiocarbonylsulfanyl-propionic acid ethyl ester and S-1-Dodecyl-S′-(α,α′-dimethyl-α″-acetic acid) trithiocarbonate chain-transfer agents (CTA), in combination with various thermal radical initiators, namely dibenzoyl peroxide and azobis(isobutyronitrile) [36,37]. The temperature was also varied (between 65 and 130 °C) and found to have an effect not only on the conversion or chain length, but also on the regularity and topology of the polymers [37]. An advantage of this method is that UV-triggered iniferter (*initiator-transfer agent-terminator*) reactions can be carried out at room temperature utilizing the above mentioned CTA, i.e., no application of external initiator is necessary, and low energy consumption can be reached [38]. NMP utilized 2-Methyl-2-[*N-tert*-butyl-*N*-(1-diethoxyphosphoryl-2,2-dimethylpropyl)-aminoxy]-*N*-propionyloxysuccinimide initiator at >100 °C. With solution polymerization using toluene and 1,4-dioxane, high regularity (~91% of 1,4-addition) could be reached, while bulk polymerization led to 80% monomer conversion with a lower portion of this microstructure [39,40]. Both reversible-deactivation radical polymerization methods have resulted in low molar mass polymyrcene (M_n ~15 kDa); only RAFT polymerization at high temperatures could produce longer chains, with poorer control over the regularity of polymers [37].

Copolymerization of *β*-myrcene with various comonomers leads to biobased amphiphilic or thermoplastic elastomeric products. The combination of styrene has particular importance from an industrial point of view, due to its similarity to styrene-butadiene rubber (SBR). Although commercially available styrene is produced mainly from petroleum resources, preparation of styrene via a biotechnological pathway has been described, employing *Escherichia coli* obtained from forestry waste using a strain of *Penicillium expansum*, in recent times. Statistical copolymerization of these two monomers was carried out via free radical copolymerization [41], and also emulsion copolymerization [18,42]. This latter, with a potassium or ammonium persulfate initiator, highlighted the effect of composition on the regioregularity. Copolymers with less than 40 mol. % styrene content had a mixed microstructure, while above this limit, only *1,4*-microstructure was obtained [42]. In this work, the determined copolymerization reactivity ratios indicated close to ideal copolymerization behavior, slightly differing from the results of free radical solution copolymerization [41]. Controlled radical polymerizations, namely RAFT and NMP, were used to synthesize statistical and block copolymers of myrcene and styrene [36,39]. The gel permeation chromatogram GPC (Figure 2) of the poly (myrcene-*b*-styrene) chain-extended block copolymer (dotted line) shifted to a lower elution time compared to its polymyrcene macroinitiator (solid line). These distinct shifts in GPC trace indicated the increase of M_n with the time of polymerization, and the results confirmed the ability of the NMP-based polymyrcene macroinitiator to reinitiate polymerization in a controlled way with styrene. Similar conditions to the homopolymerization of *β*-myrcene were used in these methods, i.e., trithiocarbonate chain-transfer agent at 65 °C, and 2-Methyl-2-[*N-tert*-butyl-*N*-(1-diethoxyphosphoryl-2,2-dimethylpropyl)-aminoxy]-*N*-propionyloxysuccinimide initiator above 100 °C, for RAFT and NMP, respectively. Miscibility of the comonomers in the polymer was confirmed by differential scanning calorimetric (DSC) measurements [36].

Aqueous emulsion cationic polymerization of styrene and *β*-myrcene, utilizing sodium dodecyl benzenesulfonate with ytterbium chloride at 40 °C, resulted in a statistical copolymer of the two comonomers, also miscible in the copolymer structure, with a molar mass range of 60–120 kDa [28]. *n*-Butyllithium-initiated anionic polymerization of *β*-myrcene and styrene, and also 4-methylstyrene, led to gradient copolymer, with solvent dependent kinetics and composition [22,43,44]. In benzene, *β*-myrcene reacted first, and styrene started to polymerize in the later stage of reaction, while in

tetrahydrofuran, the reaction turned around and started with styrene. Instead of gradient copolymer, block copolymer was also synthesized via anionic polymerization, using a *sec*-butyllithium initiator with sequential monomer addition [45]. Styrene and *α*-methyl-*p*-methyl styrene-based polymyrcene containing thermoplastic elastomers were synthesized in this second case with a phase-separated structure [23]. Coordinative chain transfer copolymerization of *β*-myrcene and styrene was carried out using half-sandwich pentamethylcyclopentadienyl-lanthanum catalyst combined with dialkyl magnesium and dialkyl aluminum, leading to a highly stereoregular copolymer with *trans-1,4*-structure, and with good yield [30]. Myrcene/styrene copolymers were also vulcanized using a standard sulfur cure system, in order to produce bio-based rubber vulcanizate for industrial applications [20,46].

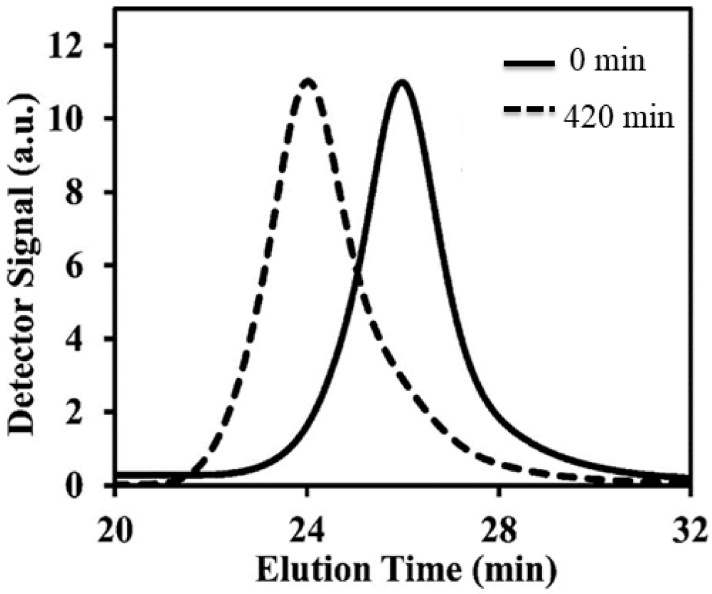

Figure 2. GPC traces of polymyrcene and its copolymer with styrene, synthesized via nitroxide-mediated radical polymerization. (Reproduced from Reference 39, with permission from American Chemical Society).

Copolymers of *β*-myrcene and isoprene/butadiene, as well as their terpolymers with styrene, were synthesized recently, too. The previously mentioned lanthanum-based catalyst for coordinative chain transfer copolymerization was also applied in the copolymerization of myrcene with isoprene and styrene, yielding polymers with stereoregular microstructures in a wide range of composition [47]. Coordination copolymerization of *β*-myrcene and isoprene with a cationic *β*-diimidosulfonate lutetium catalyst resulted in fully isotactic *3,4*-polymyrcene and polyisoprene [47]. Fine ether suspension of alkali metal between 25 and 95 °C has been used to launch copolymerization of *1,3*-butadiene and myrcene, with high conversion [48]. PN^3-Type cobalt complexes were also utilized to copolymerize *β*-myrcene with isoprene, and the resulting copolymers had predominantly *cis-1,4*-microstructure (up to 83% for myrcene). Based on the copolymer reactivity ratios in this reaction, the polymerization of isoprene was slightly favorable [49]. Interestingly, *β*-myrcene and styrene were also copolymerized with ethylene using an *ansa*-lanthanidocene catalyst, leading to a stereoregular product with an easily controllable composition [50]. Not only styrene and dienes (olefines), but also methacrylates, were combined with myrcene. Bhowmick et al. studied the copolymerization of *β*-myrcene with three different methacrylates, particularly stearyl, lauryl and butyl methacrylates, by ammonium persulfate-initiated emulsion polymerization [51]. The study stated that the length of the alkyl group in methacrylate functionality has a significant effect on the rate of propagation, i.e., the reactivity decreased with the growing side chain. The controlled radical NMP, with 2-Methyl-2-[*N-tert*-butyl-*N*-(1-diethoxyphosphoryl-2,2-dimethylpropyl)-aminoxy]-*N*-propionyloxysuccinimide initiator, has been used to copolymerize *β*-myrcene and isobornyl methacrylate, which is also a partly biobased monomer [40]. The same system has been adopted to copolymerize *β*-myrcene and glycidyl methacrylate with various feed compositions, resulting in statistical copolymers

with low dispersity ($Đ$ < 1.56) and molar mass slightly different from theoretical values [52]. A block-copolymer of these two was produced, too, capable of self-assembly. Emulsion polymerization has also been used to synthesize poly (myrcene-*co*-glycidyl methacrylate) with molar mass up to 105 kDa, including subsequent combination with non-petroleum-based silica to form a biobased nanocomposite [53]. Thermal and UV-initiated RAFT copolymerization of *β*-myrcene and poly(ethylene glycol) methyl ether methacrylate has been accomplished using a *S*,*S*-dibenzyl trithiocarbonate chain transfer agent, resulting in the introduction of 6–10 units of the hydrophilic comonomer [38]. In the first case, the reaction started with a 2,2′-Azobis(2-methylpropionitrile) thermal radical initiator at 65 °C, while for UV initiation, the iniferter method was used, and the chain transfer agent also acted as the starter.

Poly(myrcene-*co*-dibutyl itaconate) has been prepared via emulsion polymerization, initiated by ammonium persulfate, with high yield, but a tiny amount of gel fraction [54]. The monomer reactivity ratios suggest quasi-ideal copolymerization behavior of the two monomers. The produced copolymers possessed *1,4*-microstructure and were partially soluble in a wide range of organic solvents. Boron trifluoride-initiated cationic copolymerization of *β*-myrcene with tung oil has been successfully accomplished to form elastomer thermosets [55]. Dihydroxy polymyrcene, synthesized via anionic polymerization with a 3-(*tert-butyl*-dimethylsiloxy)-1-butyllithium initiator in cyclohexane, was used to polymerize lactide by ring-opening polymerization to form a triblock-copolymer elastomer [56]. Cross-linked thermosetting resins of 1,1′-(Methylenedi-4,1-phenylene)bismaleimide and myrcene were formed in 1,3-dimethyl-2-imidazolidinone at the temperatures of 150 to 250 °C, via Diels–Alder reaction [57]. Chemical modifications of myrcene, followed by radical or ionic polymerization resulting in products different from the directly polymerized polymyrcene, are not discussed here [58,59].

2.2. Polyterpene Elastomers, other Than Polymyrcene

Besides myrcene, several other terpenoids have been polymerized to elastomers. Due to the structural similarity to myrcene, the acyclic terpenes (Figure 3) can be polymerized in the same ways as the former.

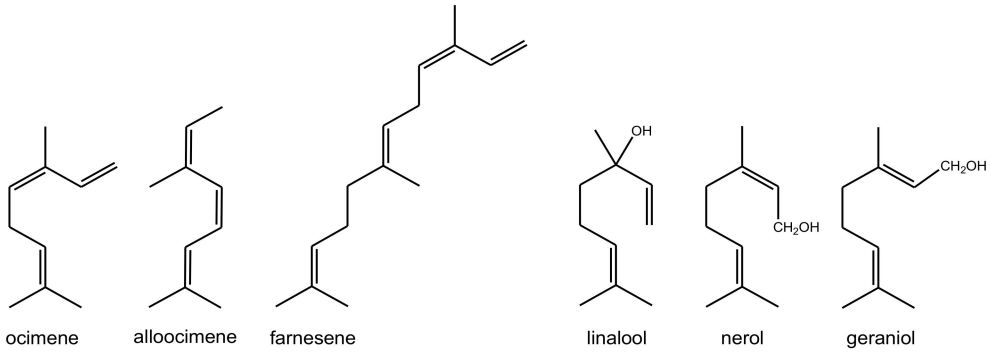

Figure 3. Structure of noncyclic terpenes and terpene alcohols, polymerized to elastomeric products.

Free radical polymerization of ocimene, using a hydrogen peroxide initiator, results in only oligomers [15]. The ionic polymerization of alloocimene has been patented. Its sodium-initiated anionic polymerization in ethers ends up in the formation of a mixture of *2,3*- and *6,7*-polyalloocimene [60]. Alloocimene polymerization with Ziegler-type (triisobutylaluminum/titanium tetrachloride or vanadium trichloride) or acid catalysts (boron fluoride etherate and titanium tetrachloride) results in preferably *4,7*-microstructures [61,62]. Ocimene and alloocimene have been polymerized by cationic polymerization using a metal halide catalyst, with at least 70% soluble fraction, that contains oligomers or polymers longer than dimers [26]. Ocimene, farnesene [63], and alloocimene [64] have been subjected to redox emulsion polymerization, using *tert*-butyl hydroperoxide and ammonium persulfate initiators, under ambient conditions. Farnesene has also been statistically copolymerized with glycidyl methacrylate, while its copolymer has been block-copolymerized with styrene, using a *N*-succinimidyl

modified commercial BlocBuilder initiator, via NMP [1]. Polymeric alloocimene via free radical method was found to be amorphous, while the rubbery polyocimene and polyfarnesene formed in low yields because of the hindered double bonds of their monomers. Ocimene was also polymerized cationically using triflate ester initiators, but the resulting oligomer had no olefinic proton detectable by ^{1}H NMR spectroscopy [27]. The anionic polymerization of farnesene in cyclohexane using a *sec*-butyllithium initiator was successfully conducted, with 85% a product of *1,4*-microstructure [65]. Alloocimene can also be copolymerized with isobutylene via quasi living carbocationic polymerization, using a trimethylpentyl chloride/$TiCl_4$ initiator/coinitiator system in a hexane/methyl chloride solvent mixture at −80 °C, resulting in thermoplastic elastomers [66–68]. Sequential polymerization using a similar system with $AlCl_3$, utilizing ethylaluminum dichloride as a coinitiator, also resulted in the formation of poly(alloocimene-*b*-isobutylene-*b*-alloocimene) thermoplastic elastomers up to 100 kDa molar mass [69].

There are also some examples of the polymerization of monoterpene alcohols, with a similar structure to the previously mentioned monomers. Dove et al. published their work recently with linalool-, nerol- and geraniol-based polyterpene resins [17]. The elastomer resins were produced using pentaerythritol tetrakis(3-mercaptopropionate) and an Irgacure 819 photo initiator, followed by postpolymerization treatments at various temperatures.

Menthol itself is not a polymerizable terpene and also acts as a radical scavenger. Menthide, a seven-membered lactone derived from menthol through Baeyer–Villiger oxidation, can be polymerized via ring-opening transesterification polymerization, using a diethylene glycol initiator and diethyl zinc/tin(II) ethylhexanoate as the catalyst (M_n up to 100 kDa) [70–73]. The resulting telechelic polymenthide was further copolymerized with other biobased monomers. After the chain-end modification of this homopolymer with triethylaluminum, lactide was polymerized with this macroinitiator [71–74]. Controllable composition and molar mass, as well as the phase-separated structure of the formed triblock-copolymer, was found. In another work, the esterification of hydroxy telechelic polymenthide (M_n ~100 kDa) resulted in dibromo functionalities, which were then applied as the macroinitiator in the atom transfer polymerization of α-methylene-γ-butyrolactone, with the final composition of 80–94 weight % terpene in the triblock copolymer [71]. A similar procedure, as in the case of menthol, was carried out for carvone (Figure 4). First, it was converted to a lactone, and then polymerized to hydroxyl telechelic polycarvomenthide using tin/diethylene glycol and zink/benzyl alcohol initiating systems, with predetermined molar mass and low polydispersity (~1.3) [75,76]. This polymer can further copolymerize with lactic acid or α-methylene-γ-butyrolactone to form triblock-copolymeric thermoset elastomers [77].

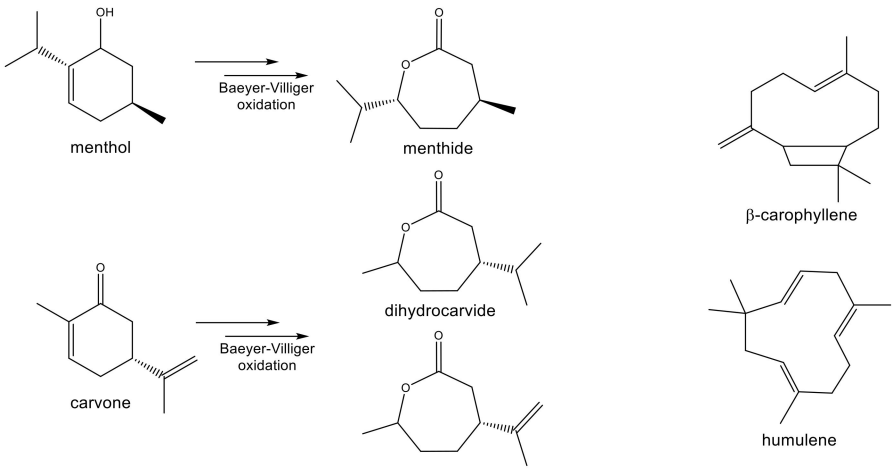

Figure 4. Synthesis and structure of some polymerizable cyclic terpenes.

β-Caryophyllene and humulene can be polymerized by ring-opening metathesis polymerization, using various Grubbs catalysts at room temperature, without modification [78]. The obtained polymers

were hydrogenated to form fully saturated renewable rubbers. Biodegradable elastomers, with high molar mass up to 250 kDa, can be produced from bile acids via ring-opening metathesis polymerization, using second generation Grubbs catalysts [79,80].

3. Properties of Polyterpene Elastomers

In this section, a brief outline of the properties of a few terpene-derived polymers, with an emphasis on β-myrcene-based homopolymers and copolymers, is presented. β-myrcene is a well-explored biobased monomer, which has reportedly been polymerized by a wide variety of polymerization techniques, producing regioselective and stereoselective products with definite properties, discussed earlier [5,10]. Goldblatt et al. showed the products obtained from the emulsion polymerization of myrcene were unusually soft and rubbery, like polymer [18]. The vulcanizates showed a tensile strength (TS) of 4.14 MPa, and an ultimate elongation or elongation at break (EAB) of 300%. The investigation into the polymerization of β-myrcene by Ziegler−Natta-type catalysts in the 1960s reported the resulting *1,4*-polymyrcenes are of relatively low molecular weight, with intrinsic viscosities of 0.3–1.0. With variation in the combination of catalysts, a higher molecular weight polymyrcene (inherent viscosities = 2 to 5.5) was obtained. The polymyrcene obtained showed tough and rubbery properties [11]. Surprisingly, after the preliminary investigation, there are no such further studies for at least 50 years into exploiting its commercial viability, or in-depth analyses of the polymer microstructure and its properties. In the early 21st century, Ritter et al. investigated the properties of polymyrcene produced via cyclodextrin complexes, using a redox initiator in aqueous media [81]. The corresponding polymer was found as water-insoluble with a glass transition temperature (T_g) of 115 °C. The formation of copolymer using myrcene and *N*-isopropyl acrylamide showed lower critical solution temperature (LCST) behavior around 80 °C in aqueous solution. The polymer obtained was water soluble with a T_g = 125 °C. The biobased polymyrcene polymer obtained using a high-temperature persulfate initiator displayed a subzero (−73 °C) glass transition temperature, along with shear-thinning behavior [19]. Polymyrcene is amorphous in nature, displaying elastomeric properties. X-ray diffraction analysis showed a typical pattern of an amorphous polymer, like natural rubber. Rheological studies revealed that the pseudoplastic behavior of polymyrcene. The mechanical properties (stress-strain plot) of the polymer showed higher TS value (97.8 kPa) and higher EAB (up to 60%), respectively, than the corresponding redox analogue (Figure 5) [19]. This was due to the presence of *3,4*- and *1,2*-vinyl microstructural defects in the case of persulfate polymyrcene, compared to the defect-free microstructure (high *1,4*-microstructure content results in much denser packing) in redox polymyrcene, which aids in higher elongation and tensile strength.

Polymyrcenes synthesized using different redox emulsion recipes displayed glass transition temperature from −70 to −58 °C, indicating a rubbery nature of the polymer. The difference in the properties of the polymers (polyterpene products) is quite contrasting, due to the variation in the percentage of microstructures [63]. Accordingly, polymyrcene polymer with a highly ordered structure, having a composition of at least 96% *1,4*-units (both *cis* and *trans*), was reported by Kali et al. The produced polyterpenes exhibited low glass transition temperature (−60 °C), reflecting the elastomeric properties of the polymer. The highly controlled molecular structures were also reflected in the results in terms of the dispersity, functionality and molar mass of the polymer [36]. The polymyrcene-*b*-polystyrene block copolymer showed a crystalline nature (T_g around 50 °C); the measured value is between the transition temperatures of two miscible polymeric phases. Polymyrcene obtained in bulk exhibits good thermal stability. The molar mass (M_n) increased linearly with the conversion to 5.5 kDa, while the polydispersity ($Đ$) remained low, around 1.3. It showed moderate weight loss below 300 °C on thermal aging, and the decomposition temperatures corresponding to 50% weight loss of polymer were observed around 385 °C [37,38].

Although in-depth investigations into the different properties of polymyrcene have been investigated, studies into the most important application performances of these polymers in the rubber industry have been lacking. Biogenic polymyrcene and poly (myrcene-*co*-styrene) elastomers were

successfully cross-linked with sulfur [46]. Amazingly, the homopolymer exhibited a good damping potential, and the copolymer showed satisfactory wet skid resistance and rolling resistance properties (Figure 6).

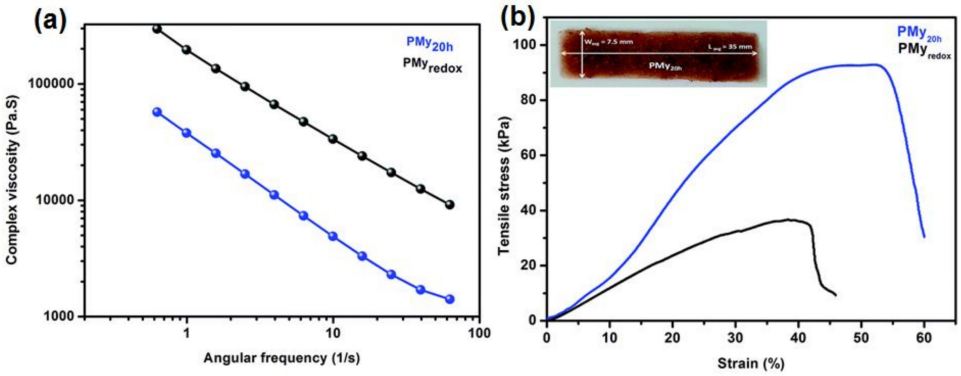

Figure 5. (**a**) Plot of complex viscosity *versus* angular frequency polymyrcene, (**b**) tensile stress-strain plot of synthesized polymyrcene. Sample designations: 'PMy_{20h}' stands for polymyrcene via persulfate polymerization, and 'PMy_{redox}' stands for polymyrcene via redox polymerization. (Reproduced from Reference 19, with permission from The Royal Society of Chemistry).

Moreover, the mechanical performance of the copolymer sufficiently improved after reinforcement with carbon black or silica-based filler (TS and EAB of 6.3 MPa, and >300% respectively) compared to pristine material (TS of 1.4 MPa, and EAB of 230%) (Figure 6) [46].

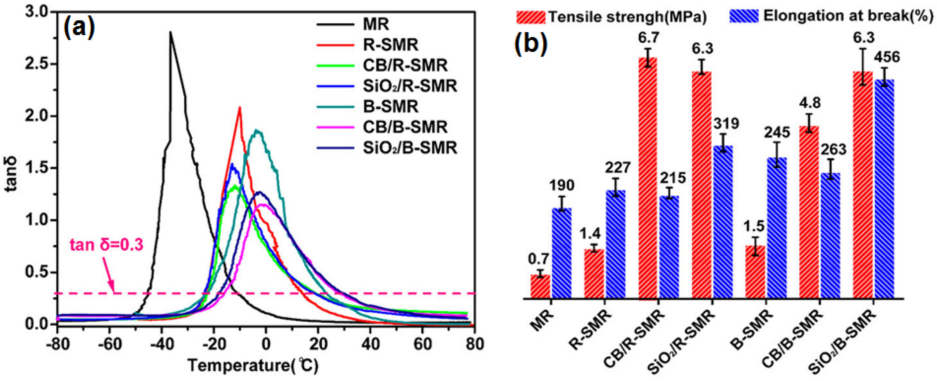

Figure 6. (**a**) Damping factor (tan δ); (**b**) Tensile strength and elongation at break of all vulcanizates. Sample designations: 'MR' stands for homopolymer of β-myrcene, 'SMR' denotes copolymer of β-myrcene and styrene, 'R and B' before SMR indicates random and block, 'CB and SiO_2' for carbon black and Silica. (Reproduced from Reference 46, with permission from American Chemical Society).

With the continuing interest and upsurge in developing sustainable polymers for potential applications in the industry, several properties and performances of β-myrcene-based copolymers have also been well explored. A triblock type thermoplastic elastomer, poly (α-methyl-*p*-methylstyrene-*b*-myrcene-*b*-α-methyl-*p*-methylstyrene), displayed micro-phase separation and impressive TS of up to 10 MPa, and ultimate EAB up to 1300% (Figure 7), as well as notably low energy loss recovery properties [23].

The copolymer, poly (myrcene-*co*-styrene), properties were mainly governed by the styrene content. The rubber vulcanizate with functional filler (carbon black) exhibited decent mechanical properties (TS of 6.4 MPa and EAB of 395%). The vulcanizate also showed improved wet skid resistance and lower rolling loss compared to a standard tire tread compound, thereby making it an appealing material for the tire industry [42]. Intending to replace butadiene in the conventional SBR solution polymerized styrene-myrcene-butadiene rubber (S-SMBR), with 100% conversion and high-molar mass

(150–200 kDa), was reported. Interestingly, the introduction of the pendant nonpolar isopropylidene group greatly improves the carbon black dispersibility in the rubber. The physico-mechanical properties of the S-SMBR vulcanizate displayed the increase of rubber's Shore A hardness from 59 to 71, and improved resilience. Furthermore, the TS and the EAB clearly tended to increase first and then decrease with the increase in the myrcene content in the vulcanizate. The TS and EAB were excellent, up to 12.60 MPa and 620% respectively, making it a promising material for the tire industry [44]. Nitroxide-mediated block-copolymerization of β-myrcene and styrene resulted in brittle thermoplastics, with strains below 20% and ultimate tensile strains well below 1 MPa, even at slow elongation rates. The statistical block copolymers displayed a range of T_g's (−77 to +30 °C) depending on myrcene molar fraction [39]. Furthermore, a β-myrcene/styrene polymer using a Lewis acid surfactant combined catalyst enables the synthesis of elastomeric materials (T_g's from −43 to +15 °C). The recycling capacity of the catalyst explored the reuse of expensive ytterbium salt, and about 70% was recovered for applying to new polymerization steps after quenching the polymer in ethanol [28]. Biobased gradient, and block-like, tapered copolymers of β-myrcene with isoprene, styrene and 4-methylstyrene, were investigated by Frey et al. The copolymers showed narrow molecular weight-distributions and two glass transition temperatures ($T_{g,1}$ = −51 to −62 °C; $T_{g,2}$ = +93 to +107 °C). Transmission Electron Microscopy (TEM) and Small-angle X-ray scattering (SAXS) measurements revealed microphase separation and highly ordered lamellar morphologies for all the polymers [43].

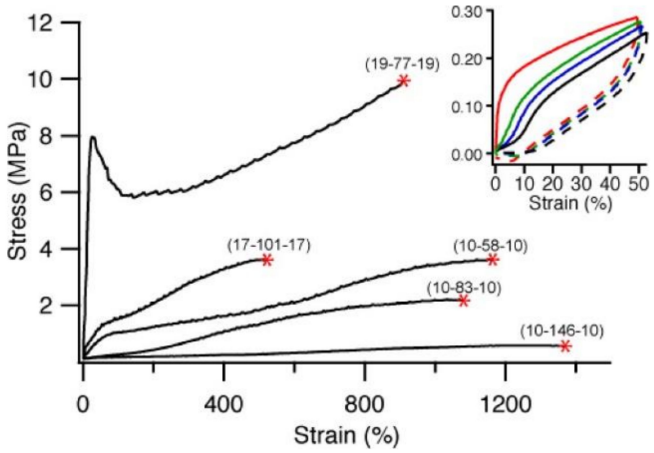

Figure 7. Representative stress-strain curves of poly (α-methyl-*p*-methylstyrene-*b*-myrcene-*b*-α-methyl-*p*-methylstyrene) samples at room temperature (* Denotes failure point). Sample designation: The sets of numbers in brackets correspond to block sizes in kg mol^{-1}; inset shows stress recovery of the 17-101-17 block copolymer. (Reproduced from Reference 23, with permission from American Chemical Society).

Highly selective polymyrcene via lanthanide-based catalyst showed a *cis*-stereoselectivity up to 98.5%, and a controlled molecular weight, reported by Loughmari et al. [29]. With changes in the combination of pre-catalyst and activator, the polymer was obtained in good yield, displaying low solubility due to the occurrence of crosslinking. However, myrcene, along with isoprene and styrene using the lanthanum half-sandwich complex, resulted in highly stereoregular statistical copolymer and terpolymer. *1,4-trans* stereoselectivity enables the growth of several stereoregular chains per catalyst, providing a significant catalyst economy [30].

Later, a series of biobased random copolymers, poly (myrcene-*co*-dibutyl itaconate), possessing a rubbery nature with scope to substitute commercial rubbers, were reported [54]. The inclusion of polar functional groups manifested good interaction with various fillers used in the rubber industry, thereby making them a judicious choice to substitute many synthetic elastomers. Sarkar et al. also delineated the properties of β-myrcene/methacrylate(s) polymers, and correlated their crystallization

behavior with respect to the side chain length of methacrylate(s) [51]. Long alkyl side chains of methacrylates dominate the thermal transitions of the copolymers to a greater extent (Figure 8).

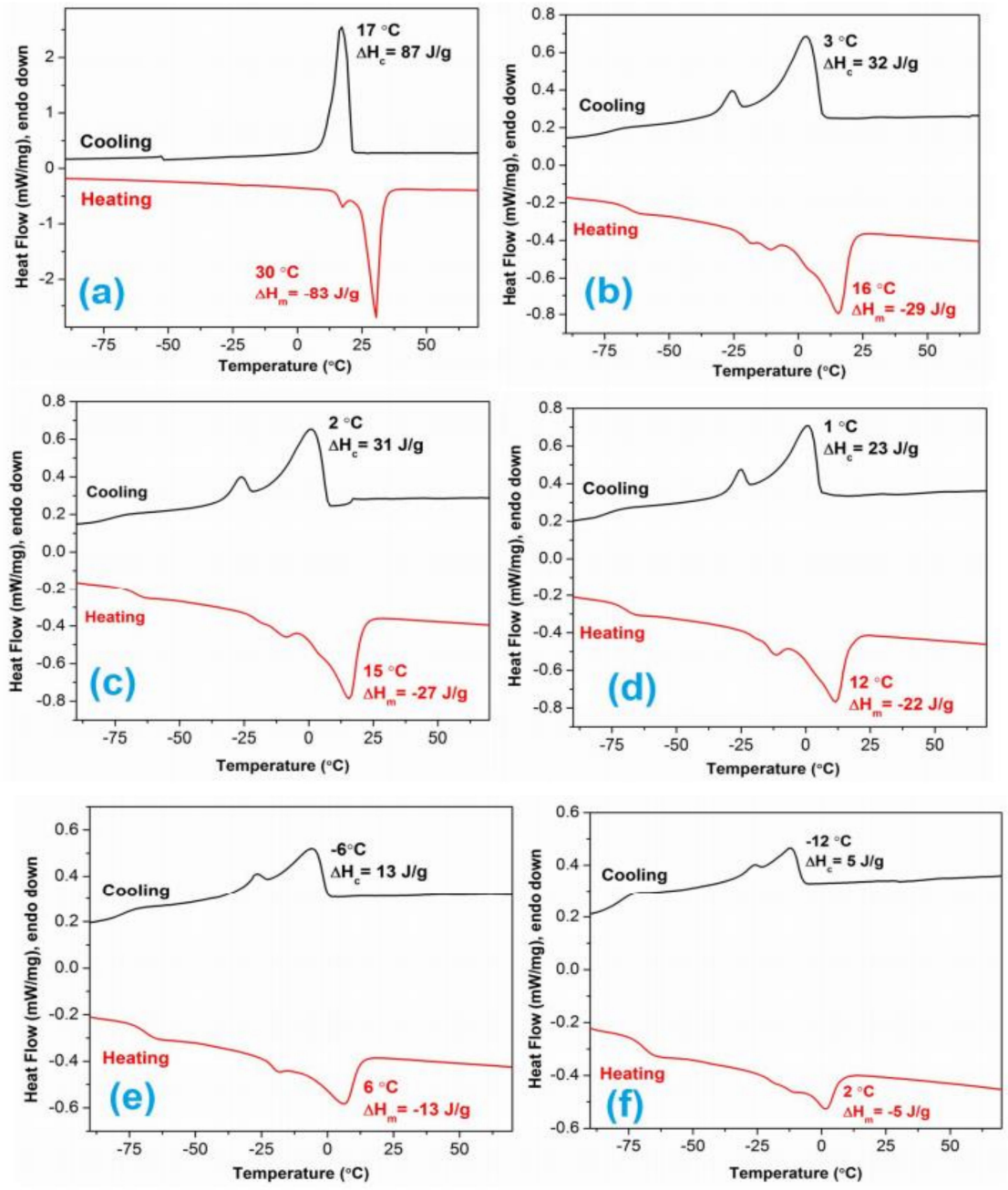

Figure 8. DSC heating and cooling traces of various stearyl methacrylate-based homo and copolymers: (**a**) poly(SM_{100}), (**b**) poly($MY_{50}SM_{50}$), (**c**) poly($MY_{60}SM_{40}$), (**d**) poly($MY_{70}SM_{30}$), (**e**) poly($MY_{80}SM_{20}$) and (f) poly($MY_{90}SM_{10}$). Sample designation: 'SM' stands for stearyl methacrylate, 'MY' denotes β-myrcene and MY:SM (value in the parentheses) indicates copolymer composition. (Reproduced from Reference 51, with permission from Wiley)

The wide-angle `X-ray diffraction` patterns confirm the amorphous nature (2θ = 12.5–25.0°) of all the copolymers. A highly reactive, epoxy group-functionalized, biobased elastomer of β-myrcene, with the ultimate aim of having a better reinforcement ability for silica-reinforced tire applications, was fabricated [53]. The copolymer of β-myrcene and glycidyl methacrylate (GMA) displayed the T_g values between −48 and −8 °C. With increasing GMA content, a decrease in polymer chain flexibility

and an increase in stiffness of the polymer was reported. The silica-filled elastomer vulcanizate exhibited better mechanical properties (TS = 2.69 MPa) than the pristine vulcanizate (TS = 1.07 MPa), due to the improvements in the reinforcement efficiency of the dispersion of silica, and the interfacial interaction between epoxy-functionalized polymer and silica (Figure 9).

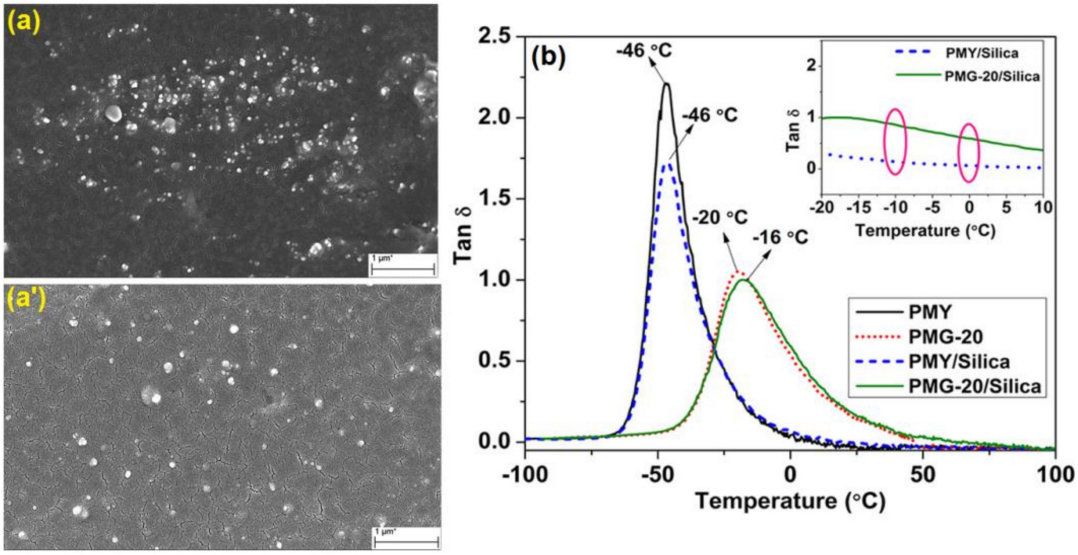

Figure 9. SEM images of (**a**,**a'**) PMY/silica and PMG-20/silica nanocomposite. (**b**) Tan δ vs. temperature plot of pristine and silica vulcanizates. Sample designations: 'PMY' stands for polymyrcene; 'PMG-20' represents copolymer containing 20 wt% GMA, PMY/Silica; and 'PMG-20/Silica' indicates silica nanocomposites. (Reproduced from Ref. 53, with permission from American Chemical Society).

Considering the polymer as an attractive choice for tire application, the vulcanizate displayed good winter traction, ice traction, and wet skid resistance properties (higher tan δ values at −20, −10, and 0 °C respectively) (Figure 9) [53]. Furthermore, β-myrcene/glycidyl methacrylate also resulted in the formation of amphiphilic statistical and diblock copolymers. The blocks exhibited microphase separation and showed two distinct T_g's. The glass transition temperature of the statistical poly (myrcene-*stat*-GMA)s increased from −77 to +43 °C [52].

Copolymerization with *L*-lactide by Zhou et al. resulted in fully biobased star polymers, displaying strains of up to 170% with elastic moduli of nearly 800 MPa. Biobased poly (β-myrcene) was used as the rubbery block and polylactide as an exterior semi-crystalline block. The mechanical properties—i.e., TS—of graft copolymers depend on the composition, particularly graft density and branch length. At the definite poly (β-myrcene) fraction, the EAB of the star comb graft copolymers was larger than the linear comb analogues [82]. The stress-strain and viscoelastic properties of β-myrcene/isobornyl methacrylate-based triblock copolymers, synthesized by SG1 nitroxide-mediated controlled radical polymerization, were elucidated [40]. Moreover, the triblock copolymer exhibited a tensile strength of 4 MPa, and an elongation at break of 500%. The phase separation of the two blocks was supported by two distinct T_g's, at about −60 °C and +180 °C, and atomic force microscopic analysis. The micro-phase separation was reported clearly with the embedding of glassy methacrylate aggregates (disperse phase) in the soft polymyrcene (continuous phase).

In continuation of the thrust to prepare terpene-derived functionalized elastomers, a new polymeric material, poly (myrcene-*co*-furfuryl methacrylate), for smart and novel application properties, has been reported [83]. With the assistance of thermal behavior, the polymer displayed excellent self-healing properties, using an external crosslinker via the Diels−Alder 'Click Chemistry' phenomenon. The healing efficiency was achieved to about 78%, shown by atomic force microscopy (AFM) depth profile imaging (Figure 10a). The copolymers showed a completely amorphous and random nature, with T_g reported between the temperature range of −40 to −25 °C (Figure 10b).

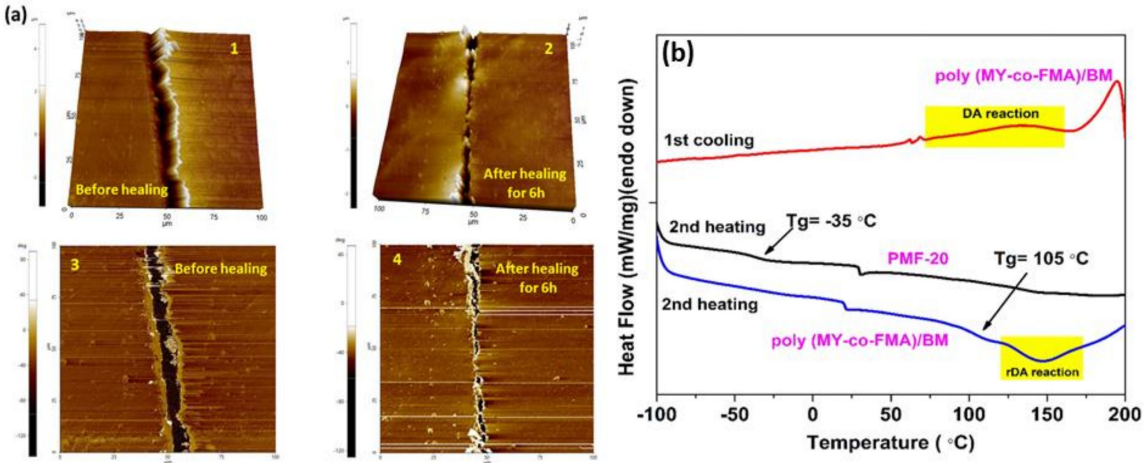

Figure 10. (**a**) Self-healing analysis by AFM imaging (1–4) of scratched and healed sample at 130 °C for 6 h. (**b**) Thermoreversibility of Diels–Alder crosslinked polymer by DSC trace. Sample designations: 'PMF-20' represents a copolymer containing 20 wt. % furfuryl methacrylate, and 'poly (MY-*co*-FMA)/BM' indicates Diels–Alder adduct. (Reproduced from Reference 83, with permission from Wiley)

Polymer networks, based on β-myrcene or β-farnesene and sunflower oil, were successfully engineered to obtain branched polymers with soft and tearable properties. Variation of T_g with sunflower oil level is shown in Figure 11a. The myrcene–oil (20/80) network presents a higher tensile modulus (97 MPa) and TS (8.8 MPa), combining high resistance and good flexibility. The materials demonstrated remarkable swelling ability in eugenol (Figure 11b), a biobased antibacterial material for coating application [84].

Dove et al. reported the use of polymyrcene polymer for 3D printing materials, in its linear and branched forms, via photo-crosslinking and subsequent functionalization with monofunctional thiols (Figure 12). Thiol-ene click chemistry on polymyrcene films for post-polymerization modification showed the difference in surface hydrophobicity of polymyrcene, from superhydrophobic, using an alkyl chain monothiol (greater than 100° water contact angle), to a hydrophilic surface displaying a water contact angle of less than 45° (Figure 13) [16].

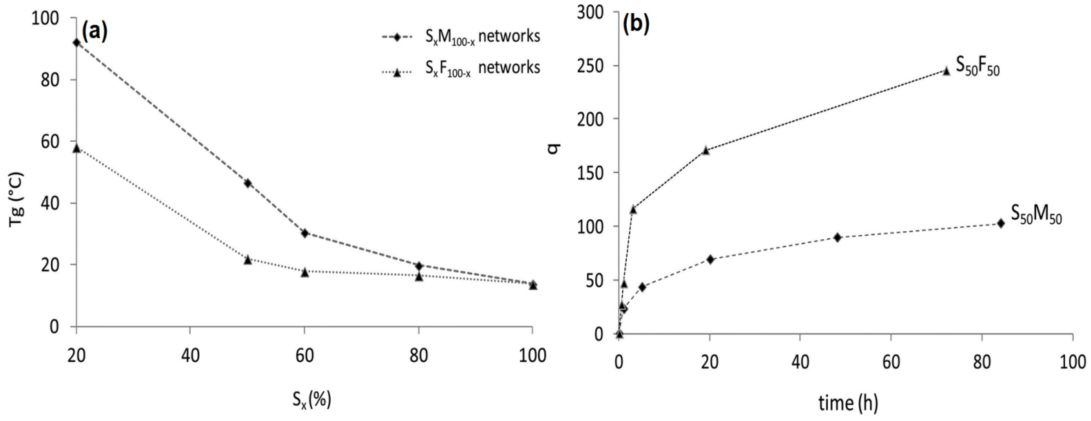

Figure 11. (**a**) Variation of T_g values with sunflower oil contents in β-myrcene and β-farnesene networks. (**b**) Swelling rate of $S_{50}M_{50}$ and $S_{50}F_{50}$ films in eugenol. Sample designations: 'S' stands for sunflower oil, 'M' represents β-myrcene, 'F' indicates β-farnesene and S:M/S:F (number in the parentheses) represents polymer network composition. (Reproduced from Reference 84, with permission from American Chemical Society).

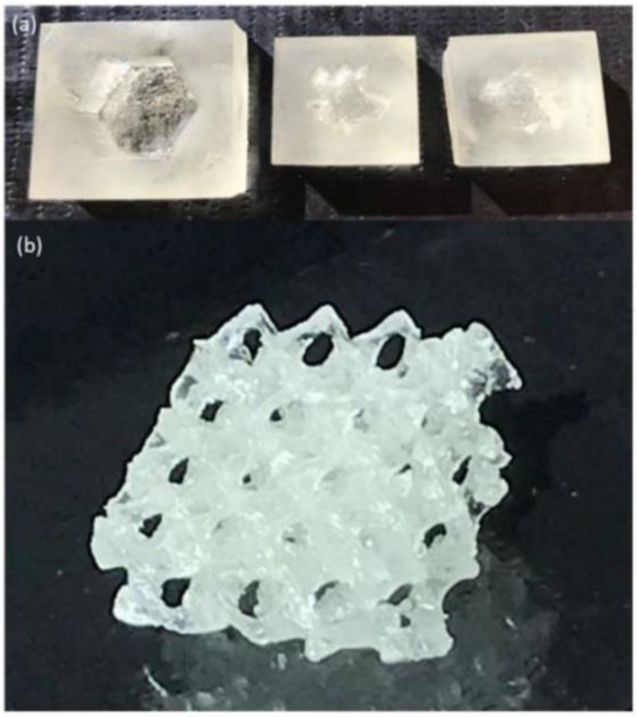

Figure 12. 3D printed models of polymyrcene resins for negative volume molds (**a**), and in porous 3D scaffolds (**b**). (Reproduced from Reference 16, with permission from American Chemical Society).

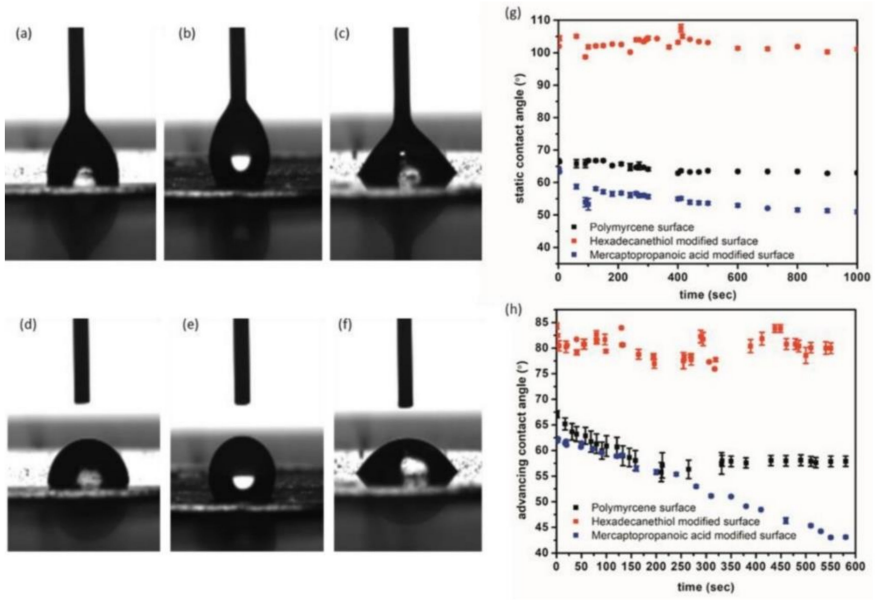

Figure 13. Goniometry comparisons of polymyrcene surfaces before (**a**,**d**) and after functionalization using hexadecanethiol (**b**,**e**) and mercaptopropanoic acid (**c**,**f**), corresponding to static (**g**) and advancing (**h**) contact angles. (Reproduced from Reference 16, with permission from American Chemical Society).

Hydroxy-functionalized polymyrcene has been put forward for use as a useful toughening agent in a highly crosslinked polyurethane. This causes improved stress-strain and impact properties, with no decrease in the T_g of the matrix and only small decreases in modulus, relative to the unmodified polyurethane network [14]. β-myrcene-based polymers were also screened as precursors for polyurethane elastomers. The study documented a range of polyurethane materials formed using hydroxy-terminated polymyrcene and modified β-myrcene diols [13,85]. The polymyrcene-based elastomers synthesized exhibited higher T_g values, ultimate elongations, and larger swelling ratios,

but were softer and possessed lower tensile strengths in comparison with elastomers based on polybutadiene [15].

In this scenario, the search for the production of synthetic rubbers is greatly expanded by the enlarging scope for using terpene-based natural synthons. Indeed, this gives an ample set of materials with promising properties. Synthesized polymers, like poly (ocimene-*co*-butadiene) and poly (farnesene-*co*-butadiene), revealed elastomeric properties along with good stereoselectivity of both butadiene (up to 95%) and terpenes (up to 92% and 86% for ocimene and farnesene, respectively) functionality [86]. The polymer with ocimene showed improved mechanical properties (stress at break = 17.81 MPa and elongation at break = 645%), and exhibited a superior performance as a component in a model tread compound, with respect to the standard butadiene (*cis*) rubbers used in tire tread application [86].

Polyalloocimene, a terpene-based rubbery-type polymer (T_g = −18 °C) obtained in 20–25% yield, was documented by Sahu et al. The research claimed that, at 35 °C in polymerization, the thermal decomposition of the polymer chains prevails, leading to a reduced molar mass of the material [64]. Polymerization of biobased *trans*-*β*-farnesene has been commercialized, producing a highly branched "bottlebrush" structure, possessing unique thermal and rheological properties. The rheological properties of the material showed that viscous behavior dominates over the frequency range. Pristine poly (*trans*-*β*-farnesene) oligomers and polymers were reported to be useful plasticizers for rubber compounds, replacing processed oils, while functionalized polyols of poly (*trans*-*β*-farnesene) can be used as intermediates in preparing polymer-like thermoplastic polyurethanes and polyurea [87].

4. Applications of Terpenes

Terpenes have been used as an essential component in various applications since antiquity. In earlier days, terpenes were used mainly as solvents in the chemical industry, but these compounds have long been used in human culture, as a component of essential oils. Terpene oils are employed widely as natural flavor additives for food, and as fragrances in perfumery (Figure 14) [1,88]. The application portfolios of terpenes also extend into conventional and alternative medicines, such as aromatherapy, and they also have anti-fungal, anti-depressant and anti-anxiety properties, as well as antiseptic, anti-bacterial and anti-inflammatory medical benefits [89]. They are also found to be an active biomaterial with antioxidant, antimicrobial/antimycotic and anticarcinogenic properties, which also support tissue regeneration and wound/tissue repair [90,91].

Most of the polyterpenes have been used as additives or tackifiers in many high-quality hot melt and pressure-sensitive adhesives, because they are compatible with many common elastomers, including natural rubber, styrene-butadiene, and styrene-isoprene rubbers, acrylics and polyolefins (including ethylene-vinyl acetate) [92,93]. The importance of polymeric myrcene is not only its biobased origin, but also its possible application potential as well. It has been recognized for its good biocompatibility, and it is approved as a food additive by the U.S. Food and Drug Administration (FDA) [10]. The utilization of bio-derived polymers is supported by recent government incentives, e.g., the United States Department of Agriculture (USDA) BioPreferred Program [94].

Nowadays, terpene-based polymers are being applied to general and engineering applications in many areas, like biodegradable packaging, antimicrobial films, coatings, fibers, or material reinforcement, as well as in medicine and pharmaceuticals [95–97]. Moreover, the use of polymyrcene polymer for smart applications, like self-healing and stimuli-responsive materials, is also a trending phenomenon [98]. These applications can be achieved either by functionalization or by post-polymerization modification, through the pendant double bonds or by using the pure polymer [42,53,83]. In combination with the great mechanical properties, the application of this elastomer, also as a copolymer, in tissue replacement or engineering would be advantageous [99]. Overall, terpene-based polymers will have increasing applications in the polymer industry in the future.

Figure 14. Meet the terpenes: a visual introduction of their uses in aroma and fragrances. Reproduced from https://www.grozine.com/2017/01/05/terpenes, accessed on March 2020).

5. Conclusions and Future Outlook

To conclude, we can say that 'sustainable development' is a hot topic in today's scientific world. In this review, different sustainable synthons and polymers from terpenes, and their applications in the current scenario of elastomer science and technology, are highlighted. In particular, significant efforts are being conducted in the field of polymer science and technology to prepare macromolecular materials utilizing terpene monomers for common, industrial and smart applications. The synthetic methodologies comprise of various polymerization techniques (to polymerize terpene-based monomers) and coupling reactions (to attach terpene entities to different synthetic polymers). We have also tried to underline several approaches that contribute towards sustainable development in the field of elastomer science and technology. Although comparisons of sustainable polymers, concerning their properties, cost and energy benefits, with their petrochemical-derived equivalents is still at an early stage, the impressive progress in this research field would surely continue to gain substantial popularity, and allure the scientific fraternity in the near future toward the attaining of its goals. These types of new green and functional materials, engineered from terpene resources, could be valued as sustainable, smart and promising materials to replace the commercial petrol-based products.

Author Contributions: Conceptualization, P.S., A.K.B. and G.K.; investigation, P.S., A.K.B. and G.K.; writing-original draft preparation, P.S., AKB and G.K.; writing-review and editing, P.S., A.K.B. and G.K.; supervision, A.K.B. and G.K. All authors have read and agreed to the published version of the manuscript.

Funding: This research received no external funding.

Acknowledgments: The authors thank IIT Kharagpur, University of Houston, and Saarland University for providing research grants and necessary facilities to carry out this work.

Conflicts of Interest: The authors declare no conflict of interest.

References

1. Breitmaier, E. *Terpenes: Flavors, Fragrances, Pharmaca, Pheromones*; Wiley-VCH Verlag GmbH: Weinheim, Germany, 2006.
2. Silvestre, A.J.; Gandini, A. Chapter 2 Terpenes: major sources, properties and applications. In *Monomers Polym. Compos. Renew. Resour*; Belgacem, M.N., Gandini, A.., Eds.; Elsevier: Amsterdam, The Netherlands, 2008; pp. 17–38.
3. Wilbon, P.A.; Chu, F.; Tang, C. Progress in renewable polymers from natural terpenes, terpenoids, and rosin. *Macromol. Rapid Commun.* **2013**, *34*, 8–37. [CrossRef] [PubMed]
4. Gandini, A.; Lacerda, T.M. From monomers to polymers from renewable resources: Recent advances. *Prog. Polym. Sci.* **2015**, *48*, 1–39. [CrossRef]
5. Zhao, J.; Schlaad, H. Synthesis of terpene-based polymers. *Adv. Polym. Sci.* **2013**, *253*, 151–190.
6. Schoenberg, E.; Marsh, H.A.; Walters, S.J.; Saltman, W.M. Polyisoprene. *Rubber Chem. Technol.* **1979**, *52*, 526–604. [CrossRef]
7. Mooibroek, H.; Cornish, K. Alternative sources of natural rubber. *Appl. Microbiol. Biotechnol.* **2000**, *53*, 355–365. [CrossRef]
8. Ouardad, S.; Deffieux, A.; Peruch, F. Polyisoprene synthesized via cationic polymerization: State of the art. *Pure Appl. Chem.* **2012**, *84*, 2065–2080. [CrossRef]
9. Moad, G. RAFT (co) polymerization of the conjugated diene monomers: Butadiene, isoprene and chloroprene. *Polym. Int.* **2017**, *66*, 26–41. [CrossRef]
10. Behr, A.; Johnen, L. Myrcene as a natural base chemical in sustainable chemistry: A critical review. *ChemSusChem* **2009**, *2*, 1072–1095. [CrossRef]
11. Marvel, C.S.; Hwa, C.C.L. Polymyrcene. *J. Polym. Sci.* **1960**, *45*, 25–34. [CrossRef]
12. Still, R.H.; Cawse, J.L.; Stanford, J.L. Functionally Terminated Polymers from Terpene Monomers and Their Applications. U.S. Patent US4564718A, 14 August 1984.
13. Cawse, J.L.; Stanford, J.L.; Still, R.H. Polymers from renewable sources. IV. Polyurethane elastomers based on myrcene polyols. *J. Appl. Polym. Sci.* **1986**, *31*, 1549–1565. [CrossRef]
14. Cawse, J.L.; Stanford, J.L.; Still, R.H. Polymers from renewable sources: 5. Myrcene-based polyols as rubber-toughening agents in glassy polyurethanes. *Polymer* **1987**, *28*, 368–374. [CrossRef]
15. Cawse, J.L.; Stanford, J.L.; Still, R.H. Polymers from renewable sources. III. Hydroxy-terminated myrcene polymers. *J. Appl. Polym. Sci.* **1986**, *31*, 1963–1975. [CrossRef]
16. Weems, A.C.; Delle Chiaie, K.R.; Yee, R.; Dove, A.P. Selective reactivity of myrcene for vat photopolymerization 3D Printing and post fabrication surface modification. *Biomacromolecules* **2020**, *21*, 163–170. [CrossRef] [PubMed]
17. Weems, A.C.; Delle Chiaie, K.R.; Worch, J.C.; Stubbs, C.J.; Dove, A.P. Terpene- and terpenoid-based polymeric resins for stereolithography 3D printing. *Polym. Chem.* **2019**, *10*, 5959–5966. [CrossRef]
18. Johanson, A.J.; McKennon, F.L.; Goldblatt, L.A. Emulsion polymerization of myrcene. *Ind. Eng. Chem.* **1948**, *40*, 500–502. [CrossRef]
19. Sarkar, P.; Bhowmick, A.K. Synthesis, characterization and properties of a bio-based elastomer: Polymyrcene. *RSC Adv.* **2014**, *4*, 61343–61354. [CrossRef]
20. Sarkar, P.; Bhowmick, A.K. Terpene-based sustainable elastomers: Vulcanization and reinforcement characteristics. *Ind. Eng. Chem. Res.* **2018**, *57*, 5197–5206. [CrossRef]
21. Ritter, H.; Steffens, C.; Storsberg, J. Cyclodextrin in polymer chemistry: Kinetic studies on the free-radical polymerization of cyclodextrin-complexed styrene from homogeneous aqueous solution. *ePolymers* **2005**, *5*, 34–37. [CrossRef]

22. Sivola, A. The *N*-butyllithium initiated polymerization of myrcene and its copolymerization with styrene. *Acta Polytech. Scand. Chem. Technol. Ser.* **1977**, *134*, 7–68.
23. Bolton, J.M.; Hillmyer, M.A.; Hoye, T.R. Sustainable thermoplastic elastomers from terpene-derived monomers. *ACS Macro Lett.* **2014**, *3*, 717–720. [CrossRef]
24. González-Villa, J.; Saldívar-Guerra, E.; León-Gómez, R.E.D.; López González, H.R.; Infante-Martínez, J.R. Kinetics of the anionic homopolymerization of β-myrcene and 4-methylstyrene in cyclohexane initiated by *n*-Butyllithium. *J. Polym. Sci. Part A Polym. Chem.* **2019**, *57*, 2157–2165.
25. Satoh, K. Controlled/living polymerization of renewable vinyl monomers into bio-based polymers. *Polym. J.* **2015**, *47*, 527–536. [CrossRef]
26. Rummersburg, A.L. Polymerized Acyclic Terpenes and Method of Production. U.S. Patent US2373419A, 10 April 1945.
27. Radchenko, A.V.; Bouchekif, H.; Peruch, F. Triflate esters as in-situ generated initiating system for carbocationic polymerization of vinyl ethers, isoprene, myrcene and ocimene. *Eur. Polym. J.* **2017**, *89*, 34–41. [CrossRef]
28. Hulnik, M.I.; Vasilenko, I.V.; Radchenko, A.V.; Peruch, F.; Ganachaud, F.; Kostjuk, S.V. Aqueous cationic homo- and co-polymerizations of β-myrcene and styrene: A green route toward terpene-based rubbery polymers. *Polym. Chem.* **2018**, *9*, 5690–5700. [CrossRef]
29. Loughmari, S.; Hafid, A.; Bouazza, A.; Bouadili, A.E.; Zinck, P.; Visseaux, M. Highly stereoselective coordination polymerization of β-myrcene from a lanthanide-based catalyst: Access to bio-sourced elastomers. *J. Polym. Sci. A Polym. Chem.* **2012**, *50*, 2898–2905. [CrossRef]
30. Georges, S.; Touré, A.O.; Visseaux, M.; Zinck, P. Coordinative chain transfer copolymerization and terpolymerization of conjugated dienes. *Macromolecules* **2014**, *47*, 4538–4547. [CrossRef]
31. Georges, S.; Bria, M.; Zinck, P.; Visseaux, M. Polymyrcene microstructure revisited from precise high-field nuclear magnetic resonance analysis. *Polymer* **2014**, *55*, 3869–3878. [CrossRef]
32. Díaz de León Gómez, R.E.; Enríquez-Medrano, F.J.; Maldonado Textle, H.; Mendoza Carrizales, R.; Reyes Acosta, K.; López González, H.R.; Olivares Romero, J.L.; Lugo Uribe, L.E. Synthesis and characterization of high *cis*-polymyrcene using neodymium-based catalysts. *Can. J. Chem. Eng.* **2016**, *94*, 823–832. [CrossRef]
33. Jia, X.; Li, W.; Zhao, J.; Yi, F.; Luo, Y.; Gong, D. Dual catalysis of the selective polymerization of biosourced myrcene and methyl methacrylate promoted by salicylaldiminato cobalt(II) complexes with a pendant donor. *Organometallics* **2019**, *38*, 278–288. [CrossRef]
34. Braunecker, W.A.; Matyjaszewski, K. Controlled/living radical polymerization: Features, developments, and perspectives. *Prog. Polym. Sci.* **2007**, *32*, 93–146. [CrossRef]
35. Grubbs, R.B. Nitroxide-mediated radical polymerization: limitations and versatility. *Polym. Rev.* **2011**, *51*, 104–137. [CrossRef]
36. Hilschmann, J.; Kali, G. Bio-based polymyrcene with highly ordered structure via solvent free controlled radical polymerization. *Eur. Polym. J.* **2015**, *73*, 363–373. [CrossRef]
37. Bauer, N.; Brunke, J.; Kali, G. Controlled radical Polymerization of myrcene in bulk: Mapping the effect of conditions on the system. *ACS Sustain. Chem. Eng.* **2017**, *5*, 10084–10092. [CrossRef]
38. Niedner, L.; Kali, G. Green engineered polymers: Solvent free, room-temperature polymerization of monomer from a renewable resource, without utilizing initiator. *Chem. Select* **2019**, *4*, 3495–3499. [CrossRef]
39. Métafiot, A.; Kanawati, Y.; Gérard, J.-F.; Defoort, B.; Marić, M. Synthesis of β-myrcene-based polymers and styrene block and statistical copolymers by SG1 nitroxide-mediated controlled radical polymerization. *Macromolecules* **2017**, *50*, 3101–3120. [CrossRef]
40. Métafiot, A.; Gagnon, L.; Pruvost, S.; Hubert, P.; Gérard, J.-F.; Defoort, B.; Marić, M. β-myrcene/isobornyl methacrylate SG1 nitroxide-mediated controlled radical polymerization: Synthesis and characterization of gradient, diblock and triblock copolymers. *RSC Adv.* **2019**, *9*, 3377–3395. [CrossRef]
41. Trumbo, D.L. Free radical copolymerization behavior of myrcene. *Polym. Bull.* **1993**, *31*, 629–636. [CrossRef]
42. Sarkar, P.; Bhowmick, A.K. Terpene based sustainable elastomer for low rolling resistance and improved wet grip application: Synthesis, characterization and properties of poly (styrene-*co*-myrcene). *ACS Sustain. Chem. Eng.* **2016**, *4*, 5462–5474. [CrossRef]
43. Grune, E.; Bareuther, J.; Blankenburg, J.; Appold, M.; Shaw, L.; Müller, A.H.E.; Floudas, G.; Hutchings, L.R.; Gallei, M.; Frey, H. Towards bio-based tapered block copolymers: The behaviour of myrcene in the statistical anionic copolymerization. *Polym. Chem.* **2019**, *10*, 1213–1220. [CrossRef]

44. Zhang, J.; Lu, J.; Su, K.; Wang, D.; Han, B. Bio-based β-myrcene-modified solution-polymerized styrene-butadiene rubber for improving carbon black dispersion and wet skid resistance. *J. Appl. Polym. Sci.* **2019**, *136*, 48159–48169. [CrossRef]
45. Quirk, R.P.; Huang, T.-L. Alkyllithium-initiated polymerization of myrcene new block copolymers of styrene and myrcene. In *New Monomers and Polymers*; Springer: Boston, MA, USA, 1984; pp. 329–355.
46. Zhang, S.; Han, L.; Ma, H.; Liu, P.; Shen, H.; Lei, L.; Li, C.; Yang, L.; Li, Y. Investigation on synthesis and application performance of elastomers with biogenic myrcene. *Ind. Eng. Chem. Res.* **2019**, *58*, 12845–12853. [CrossRef]
47. Liu, B.; Li, L.; Sun, G.; Liu, D.; Li, S.; Cui, D. Isoselective 3,4- (co)polymerization of bio-renewable myrcene using NSN-ligated rare-earth metal precursor: An approach to a new elastomer. *Chem. Commun.* **2015**, *51*, 1039–1041. [CrossRef] [PubMed]
48. Gleason, A.H.; Nelson, J.F. Synthetic Drying Oils by Copolymerization of Diolefins with Myrcene. U.S. Patent 2829065, 1 April 1958.
49. Li, W.; Zhao, J.; Zhang, X.; Gong, D. Capability of PN^3-type cobalt complexes toward selective (Co-)polymerization of myrcene, butadiene, and isoprene: Access to biosourced polymers. *Ind. Eng. Chem. Res.* **2019**, *58*, 2792–2800. [CrossRef]
50. Laur, E.; Welle, A.; Vantomme, A.; Brusson, J.M.; Carpentier, J.F.; Kirillov, E. Stereoselective copolymerization of styrene with terpenes catalyzed by an Ansa-lanthanidocene catalyst: Access to new syndiotactic polystyrene-based materials. *Catalysts* **2017**, *7*, 361. [CrossRef]
51. Sarkar, P.; Bhowmick, A.K. Terpene based sustainable methacrylate copolymer series by emulsion polymerization: Synthesis and structure-property relationship. *J. Polym. Sci. Part A Polym. Chem.* **2017**, *55*, 2639–2649. [CrossRef]
52. Métafiot, A.; Gérard, J.-F.; Defoort, B.; Marić, M. Synthesis of β-myrcene/glycidyl methacrylate statistical and amphiphilic diblock copolymers by SG1 nitroxide-mediated controlled radical polymerization. *J. Polym. Sci. Part A Polym. Chem.* **2018**, *56*, 860–878. [CrossRef]
53. Sahu, P.; Sarkar, P.; Bhowmick, A.K. Design of a molecular architecture via a green route for an improved silica reinforced nanocomposite using bioresources. *ACS Sustain. Chem. Eng.* **2018**, *6*, 6599–6611. [CrossRef]
54. Sarkar, P.; Bhowmick, A.K. Green approach toward sustainable polymer: Synthesis and characterization of poly-(myrcene-*co*-dibutyl itaconate). *ACS Sustainable Chem. Eng.* **2016**, *4*, 2129–2141. [CrossRef]
55. Sibaja, B.; Sargent, J.; Auad, M.L. Renewable thermoset copolymers from tung oil and natural terpenes. *J. Appl. Polym. Sci.* **2014**, *131*, 41155–41162. [CrossRef]
56. Zhou, C.; Wei, Z.; Lei, X.; Li, Y. Fully biobased thermoplastic elastomers: Synthesis and characterization of poly(L-lactide)-*b*-polymyrcene-*b*-poly(L-lactide) triblock copolymers. *RSC Adv.* **2016**, *6*, 63508–63514. [CrossRef]
57. Shibata, M.; Asano, M. Biobased thermosetting resins composed of terpene and bismaleimide. *J. Appl. Polym. Sci.* **2013**, *129*, 301–309. [CrossRef]
58. Kobayashi, S.; Lu, C.; Hoye, T.R.; Hillmyer, M.A. Controlled polymerization of a cyclic diene prepared from the ring-closing metathesis of a naturally occurring monoterpene. *J. Am. Chem. Soc.* **2009**, *131*, 7960–7961. [CrossRef] [PubMed]
59. Firdaus, M.; Espinosa, L.M.; Meier, M.A.R. Terpene-based renewable monomers and polymers via thiol-ene additions. *Macromolecules* **2011**, *44*, 7253–7262. [CrossRef]
60. Veazey, R.L. Polyalloocimene and Method for the Preparation Thereof. U.S. Patent 4694059, 15 September 1987.
61. Marvel, C.S.; Kiener, P.E.; Vessel, E.D. Polyalloöcimene. *J. Am. Chem. Soc.* **1959**, *81*, 4694–4697. [CrossRef]
62. Marvel, C.S.; Kiener, P.E. Polyalloöcimene II. *J. Polym. Sci.* **1962**, *61*, 311–331. [CrossRef]
63. Sahu, P.; Bhowmick, A.K. Redox emulsion polymerization of terpenes: Mapping the effect of the system, structure, and reactivity. *Ind. Eng. Chem. Res.* **2019**, *58*, 20946–20960. [CrossRef]
64. Sahu, P.; Sarkar, P.; Bhowmick, A.K. Synthesis and characterization of a terpene-based sustainable polymer: Poly-alloocimene. *ACS Sustain. Chem. Eng.* **2017**, *5*, 7659–7669. [CrossRef]
65. Newmark, R.A.; Majumdar, R.N. ^{13}C-NMR spectra of *cis*-polymyrcene and *cis*-polyfarnesene. *J. Polym. Sci. A Polym. Chem.* **1988**, *26*, 71–77. [CrossRef]
66. Gergely, A.L.; Turkarslan, O.; Puskas, J.E.; Kaszas, G. The role of electron pair donors in the carbocationic copolymerization of isobutylene with alloocimene. *J. Polym. Sci. Part A Polym. Chem.* **2013**, *51*, 4717–4721. [CrossRef]

67. Gergely, A.L.; Puskas, J.E. Synthesis and characterization of thermoplastic elastomers with polyisobutylene and polyalloocimene blocks. *J. Polym. Sci. A Polym. Chem.* **2015**, *53*, 1567–1574. [CrossRef]
68. Roh, J.H.; Roy, D.; Lee, W.K.; Gergely, A.L.; Puskas, J.E.; Roland, C.M. Thermoplastic elastomers of alloocimene and isobutylene triblock copolymers. *Polymer* **2015**, *56*, 280–283. [CrossRef]
69. Kantor, J.; Puskas, J.E.; Kaszas, G. The effect of reaction conditions on the synthesis of thermoplastic elastomers containing polyalloocimene, polyisobutylene and tapered blocks. *Chin. J. Polym. Sci.* **2019**, *37*, 884–890. [CrossRef]
70. Zhang, D.; Hillmyer, M.A.; Tolman, W.B. Catalytic polymerization of a cyclic ester derived from a "cool" natural precursor. *Biomacromolecules* **2005**, *6*, 2091–2095. [CrossRef] [PubMed]
71. Shin, J.; Lee, Y.; Tolman, W.B.; Hillmyer, M.A. Thermoplastic elastomers derived from menthide and tulipalin A. *Biomacromolecules* **2012**, *13*, 3833–3840. [CrossRef]
72. Wanamaker, C.L.; O'Leary, L.E.; Lynd, N.A.; Hillmyer, M.A.; Tolman, W.B. Renewable-resource thermoplastic elastomers based on polylactide and polymenthide. *Biomacromolecules* **2007**, *8*, 3634–3640. [CrossRef]
73. Shin, J.; Martello, M.T.; Shrestha, M.; Wissinger, J.E.; Tolman, W.B.; Hillmyer, M.A. Pressure-sensitive adhesives from renewable triblock copolymers. *Macromolecules* **2011**, *44*, 87–94. [CrossRef]
74. Wanamaker, C.L.; Bluemle, M.J.; Pitet, L.M.; O'Leary, L.E.; Tolman, W.B.; Hillmyer, M.A. Consequences of polylactide stereochemistry on the properties of polylactide-polymenthide-polylactide thermoplastic elastomers. *Biomacromolecules* **2009**, *10*, 2904–2911. [CrossRef]
75. Yang, J.; Lee, S.; Choi, W.J.; Seo, H.; Kim, P.; Kim, G.-J.; Kim, Y.-W.; Shin, J. Thermoset elastomers derived from carvomenthide. *Biomacromolecules* **2015**, *16*, 246–256. [CrossRef]
76. Lowe, J.R.; Martello, M.T.; Tolman, W.B.; Hillmyer, M.A. Functional biorenewable polyesters from carvone-derived lactones. *Polym. Chem.* **2011**, *2*, 702–708. [CrossRef]
77. Jang, J.; Park, H.; Jeong, H.; Mo, E.; Kim, Y.; Yuk, J.S.; Choi, S.Q.; Kim, Y.-W.; Shin, J. Thermoset elastomers covalently crosslinked by hard nanodomains of triblock copolymers derived from carvomenthide and lactide: Tunable strength and hydrolytic degradability. *Polym. Chem.* **2019**, *10*, 1245–1257. [CrossRef]
78. Grau, E.; Mecking, S. Polyterpenes by ring opening metathesis polymerization of caryophyllene and humulene. *Green Chem.* **2013**, *15*, 1112–1115. [CrossRef]
79. Gautrot, J.E.; Zhu, X.X. Main-Chain Bile Acid based degradable elastomers synthesized by entropy-driven ring-opening metathesis polymerization. *Angew. Chem. Int. Edit.* **2006**, *45*, 6872–6874. [CrossRef] [PubMed]
80. Gautrot, J.E.; Zhu, X.X. Macrocyclic bile acids: From molecular recognition to degradable biomaterial building blocks. *J. Mater. Chem.* **2009**, *19*, 5705–5716. [CrossRef]
81. Choi, S.W.; Ritter, H. Novel polymerization of myrcene in aqueous media via cyclodextrin-complexes. *ePolymers* **2007**, *45*, 1–8. [CrossRef]
82. Zhou, C.; Wei, Z.; Wang, Y.; Yu, Y.; Leng, X.; Li, Y. Fully biobased thermoplastic elastomers: Synthesis of highly branched star comb poly(β-myrcene)-graft-poly(l-lactide) copolymers with tunable mechanical properties. *Eur. Polym. J.* **2018**, *99*, 477–484. [CrossRef]
83. Sahu, P.; Bhowmick, A.K. Sustainable self-healing elastomers with thermoreversible network derived from biomass via emulsion polymerization. *J. Polym. Sci. Part A Polym. Chem.* **2019**, *57*, 738–751. [CrossRef]
84. Mangeon, C.; Thevenieau, F.; Renard, E.; Langlois, V. Straightforward route to design biorenewable networks based on terpenes and sunflower oil. *ACS Sustainable Chem. Eng.* **2017**, *5*, 6707–6715. [CrossRef]
85. Cawse, J.L.; Stanford, J.L. Rubber-toughened polyurethane network and composite materials. *Polymer* **1987**, *28*, 356–367. [CrossRef]
86. Lamparelli, D.H.; Paradiso, V.; Della Monica, F.; Proto, A.; Guerra, S.; Giannini, L.; Capacchione, C. Toward more sustainable elastomers: Stereoselective copolymerization of linear terpenes with butadiene. *Macromolecules* **2020**, *53*, 1665–1673. [CrossRef]
87. Yoo, T.; Henning, S.K. Synthesis and characterization of farnesene-based polymers. *Rubber Chem. Technol.* **2017**, *90*, 308–324. [CrossRef]
88. Leavell, M.D.; McPhee, D.J.; Paddon, C.J. Developing fermentative terpenoid production for commercial usage. *Curr. Opin. Biotechnol.* **2016**, *37*, 114–119. [CrossRef] [PubMed]
89. Bass, S. What Are Terpenes? Outlining their History, Properties, and Functions. Available online: http://www.herbanindigo.com/cannabis/p/what-are-terpenes (accessed on 15 May 2019).
90. Hazan, Z. Therapeutic Uses of Mastic Gum Fractions. U.S. Patent WO2010100650A2, 10 September 2010.
91. Hazan, Z.; Amselem, S. Compositions of Polymeric Myrcene. U.S. Patent WO2010100651A2, 10 September 2010.

92. Wypych, G. *Handbook of Surface Improvement and Modification*; ChemTec Publishing: Toronto, ON, Canada, 2018.
93. Rubulotta, G.; Quadrelli, E.A. Terpenes: A valuable family of compounds for the production of fine chemicals. In *Studies in Surface Science and Catalysis*; Elsevier: Amsterdam, The Netherlands, 2019; pp. 215–229.
94. United States Department of Agriculture. USDA BioPreferred Program Guidelines How to Display and Promote the USDA Biobased Product Label, June 2016. Available online: https://www.biopreferred.gov/BPResources/files/BioPreferredBrandGuide.pdf (accessed on 1 June 2019).
95. Papageorgiou, G.Z. Thinking green: Sustainable polymers from renewable resources. *Polymers* **2018**, *10*, 952. [CrossRef] [PubMed]
96. Miller, S.A. Sustainable polymers: Opportunities for the next decade. *ACS Macro Lett.* **2013**, *2*, 550–554. [CrossRef]
97. Schneiderman, D.K.; Hillmyer, M.A. 50th anniversary perspective: There is a great future in sustainable polymers. *Macromolecules* **2017**, *50*, 3733–3749. [CrossRef]
98. Herbert, K.M.; Schrettl, S.; Rowan, S.J.; Weder, C. 50th anniversary perspective: Solid-state multistimuli, multiresponsive polymeric materials. *Macromolecules* **2017**, *50*, 8845–8870. [CrossRef]
99. Hazan, Z.; Adamsky, K.; Lucassen, A.C.B. Use of Isolated Fractions of Mastic Gum for Treating Optic Neuropathy. U.S. Patent WO2016142936A1, 15 September 2016.